# Fatigue delamination behaviour of carbon fibre/epoxy composites interleaved with thermoplastic veils

Quan, Dong; Murphy, Neal; Ivanković, Alojz; Zhao, Guoqun; Alderliesten, René

**DOI**
10.1016/j.compstruct.2021.114903

**Publication date**
2021

**Document Version**
Final published version

**Published in**
Composite Structures

Composite Structures 281 (2022) 114903

Contents lists available at ScienceDirect

Composite Structures

journal homepage: www.elsevier.com/locate/compstruct

# Fatigue delamination behaviour of carbon fibre/epoxy composites interleaved with thermoplastic veils

Dong Quan [a,*], Neal Murphy [b], Alojz Ivanković [b], Guoqun Zhao [a], René Alderliesten [c]

[a] Key Laboratory for Liquid–Solid Structural Evolution and Processing of Materials (Ministry of Education), Shandong University, China
[b] School of Mechanical and Materials Engineering, University College Dublin, Ireland
[c] Department of Aerospace Structures and Materials, Delft University of Technology, Netherlands

ARTICLE INFO

*Keywords:*
Interlay toughening
Fatigue delamination
Thermoplastic fibres
Toughening mechanism

ABSTRACT

Interleaving thermoplastic veils has proved to enhance the interlaminar fracture toughness of carbon fibre/epoxy composites under static loading conditions. However, the fatigue delamination behaviour has yet to be investigated. Herein, meltable Polyamide-12 (PA) veils and non-meltable Polyphenylene-sulphide (PPS) veils were used for interlay toughening of unidirectional (UD) and non-crimp fabric (NCF) laminates that were manufactured using a prepreg process and resin transfer moulding process, respectively. The results of Mode-I fatigue delamination tests demonstrated a significant improvement in the fatigue life of the laminates due to interleaving. Additionally, the fatigue resistance energy has been maximumly increased by 143% and 190% for the UD and NCF laminates, respectively. The microscopy analysis revealed that the toughening mechanisms of thermoplastic veils were affected by the form of the thermoplastic veils in the laminates (melted or non-melted), the fracture mechanisms of the reference laminates and the adhesion/miscibility between the thermoplastic veils and the epoxy.

## 1. Introduction

Carbon fibre reinforced polymers are widely used in structural applications due to their light weight, high mechanical properties and excellent structural performance. Epoxy resins are the most widely used matrix of thermosetting composites due to their high modulus, high strength, low creep and excellent thermal stability. However, carbon fibre reinforced epoxy composites (CF/EPs) are prone to interply delamination, owing to the brittleness of the epoxy matrix and the laminated structure of the composites. Accordingly, enhancing the interlaminar fracture properties of CF/EPs has been a research focus over the last two decades.

Adding toughening layers between the plies of CF/EPs or interlay toughening is an easy process that does not necessarily add significant cost and manufacturing difficulties to the laminates. For this reason, it has attracted considerable attention from both academics and industrialists. To date, many types of materials have been used for interlay toughening of CF/EPs, such as chopped carbon fibres [1], carbon nanomaterials [2], stainless steel fibres [3], thermoplastic films [4] and thermoplastic veils [5]. In general, the toughening efficiency of the interleaving technique depends on the type and amount of the interlayer materials. Among different interlayer materials, the tough, ductile, porous and lightweight nature of thermoplastic veils makes them outstanding candidates for toughening CF/EPs. Extensive research, including [6–13] has proved that interlaying thermoplastic veils could significantly improve the interlaminar fracture properties of CF/EPs. Moreover, many studies reported that the addition of thermoplastic veils into CF/EPs had no detrimental effects to the other mechanical properties, such as flexural modulus and strength [6,14–16] and interlaminar shear strength [6–8,15]. This is another advantage of using thermoplastic veils as interlayer materials of CF/EPs.

To date, a significant number of studies have been carried out to investigate the effects of the areal density of the veils [6,7,17–19], the veil material [11,17,20,21], the form of the veils in the FRPs, i.e. melted or non-melted [11,14], and the architecture of the carbon fibre fabrics [12,19–21] on the fracture properties of the interleaved CF/EPs. However, the majority of these studies focused on the fracture behaviour of the laminates under static loading conditions. Only a limited number of publications, including [22–24] reported the effects of interleaving thermoplastic veils on the fatigue delamination behaviour of CF/EPs. Brugo et al. [23,24] studied the mode-I fatigue delamination behaviour of a plain weave CF/EP interleaved with 18 g/m$^2$ Nylon veils. It was observed that the addition of interlayers significantly increased the delamination toughness by over 100% and lowered the crack propagation rate by 36-27 times under fatigue loading conditions.

* Corresponding author.
*E-mail address:* quandong@sdu.edu.cn (D. Quan).

https://doi.org/10.1016/j.compstruct.2021.114903
Received 8 June 2021; Accepted 26 October 2021
Available online 27 November 2021

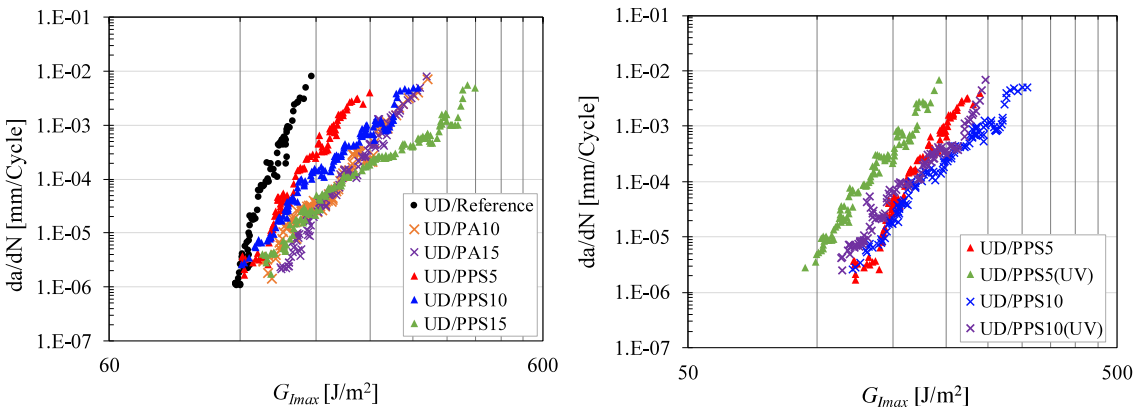


(a) Original veils (b) Effects of UV treatment

**Fig. 1.** The Paris representation of FDG of the interleaved UD laminates.

Daelemans et al. [22] investigated the mode-II fatigue delamination behaviour of CF/EPs interleaved with different thermoplastic veils. Improved fatigue delamination resistance was observed for all three nanofibre types tested, i.e. polycaprolactone (PCL), polyamide 6 (PA 6) and polyamide 6.9 (PA 6.9), with the PCL interleaved laminates exhibiting the best performance. The different toughening performance of different veils was attributed to the different veil/epoxy interface adhesion, that subsequently affected the toughening mechanisms of the veils. While all these studies reported improvements in the fatigue delamination behaviour, further research is still needed to fully address the fatigue delamination behaviour and toughening mechanisms of interleaved CF/EPs.

In our previous work [25–27], the fracture behaviour of CF/EPs interleaved with thermoplastic veils under static loading conditions was systematically investigated. Significant improvements in the mode-I and mode-II fracture energies of the CF/EPs were observed in all cases, with the toughening levels affected by the areal density and material type of the veils, the adhesion at the veil/epoxy interface, the form of the veils within the laminates (melted or non-melted) and the architecture of the carbon fibres. This work aims to investigate the effects of interlaying thermoplastic veils on the fatigue delamination behaviour of the CF/EPs. The laminates used were a unidirectional (UD) laminate manufactured from CF/EP prepreg and a non-crimp fabric (NCF) laminate produced by a resin transfer moulding (RTM) process, and thermoplastic veils based on PPS and PA12 were used as interlayers. These two laminates were chosen because they exhibited significantly different fracture mechanisms under static loading conditions, which subsequently affected the toughening mechanisms of the thermoplastic veils [25,26]. The fatigue delamination behaviour of the interleaved laminates was studied, and the toughening mechanisms were also investigated.

## 2. Experimental

### 2.1. Materials and sample preparation

The UD laminates were based on carbon fibre/epoxy prepreg (HYE-1034E from Cytec, Solvay Group). The NCF laminates were manufactured by a RTM process, using Toray T700Sc-50C biaxial fabric from Saertex GmbH and CYCOM 890RTM resin from Cytec, Solvay Group. The same curing schedule was used for both laminates, i.e. at 180 °C under a pressure of 0.5 MPa for 90 mins. Thermoplastic veils based on Polyphenylene sulphide (PPS) and PA12 were supplied by Technical Fibre Products Ltd., UK. They were inserted at the mid-plane of the laminates during the layup process. It should be noted that the PA fibres melted and the PPS fibres remained in their fibrous form during the laminate curing process [25]. PPS veils treated by UV light (Light Hammer 6 from Heraeus Noblelight, UK) for 10 s were also used as interlayers, to investigate the effects of the veil/epoxy adhesion on the fatigue delamination behaviour of the CF/EPs. This treatment process has proved to significantly increase the adhesion between the PPS veils and epoxy matrix in our previous work [27]. After the laminates were cured in an in-house press-clave, double cantilever beam (DCB) specimens with a width of 20 mm and a length of 160 mm were machined out. Additional information on the materials and sample preparation can be found in [25].

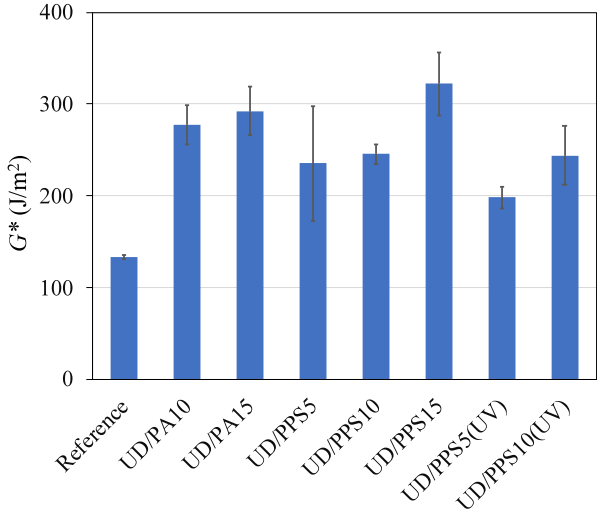


**Fig. 2.** Fatigue resistance energy ($G^*$) of the interleaved UD laminates.

### 2.2. Fatigue delamination growth test

The fatigue delamination growth (FDG) test on the DCB specimens was carried out on a 10 kN MTS machine under displacement control. The DCB specimens were firstly pre-cracked under static loading conditions to determine the maximum displacement for the FDG test. During the FDG tests, a displacement ratio of 0.1 was used, at a cyclic loading frequency of 10 Hz. The crack growth was monitored using a computer controlled digital camera system at the maximum displacement, while the load, displacement and cycle numbers were automatically stored every 100 cycles. Three specimens were tested for each set.

The Paris relation between the crack propagation rate per cycle, $da/dN$, and the maximum energy release rate, $G_{Imax}$ was used to analyse the FDG behaviour of the laminates. In this work, $G_{Imax}$ was calculated using a modified compliance calibration method [28] according

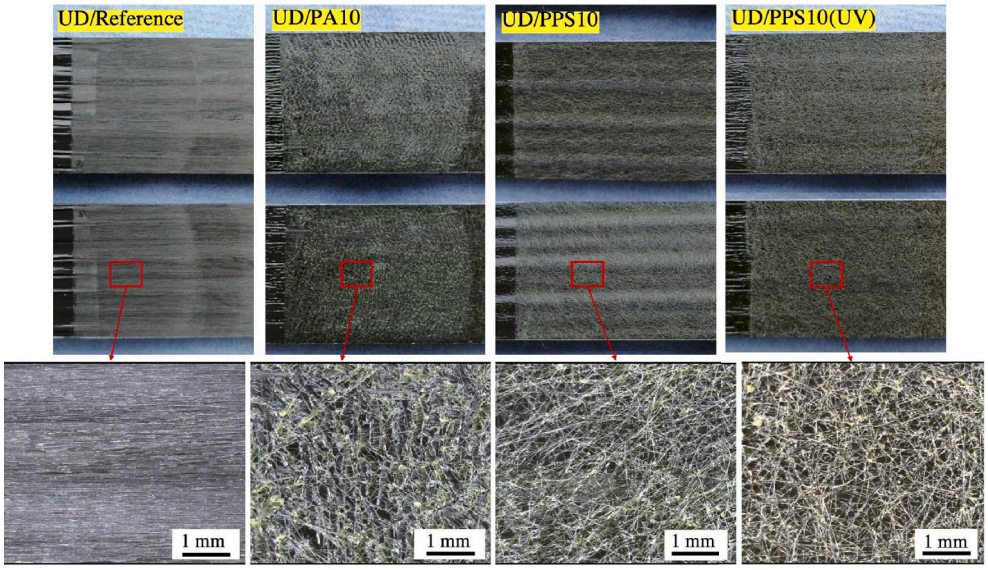


(a) Images of the fracture surface

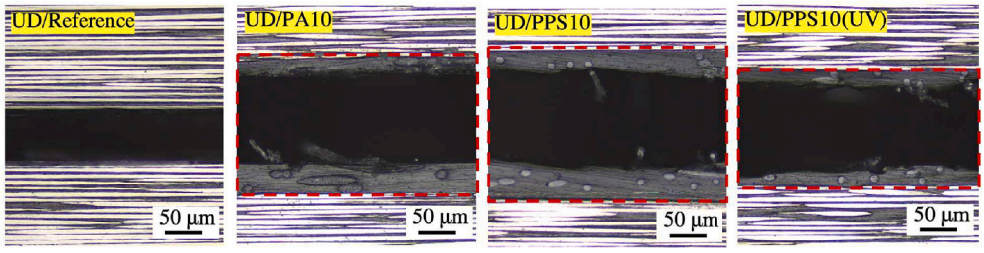


(b) Side view of the crack path

**Fig. 3.** Representative images of the fatigue fracture surface and side-view of the crack path of the UD laminates. The red dashed boxes in (b) indicate the interlayers.

to the following equation:

$$G_I = \frac{3P^2C^{2/3}}{2A_1Bh} \tag{1}$$

where $P$ is the applied load, $C$ is the compliance of the DCB specimen, $B$ and $h$ are the width and thickness of the specimens and $A_1$ is the slope of the $a/h$ against $C^{1/3}$ curve. $da/dN$ was determined using the 7-point Increment Polynomial Method [29].

The actual strain energy release rate of the DCB specimens was also calculated, which is defined as:

$$G^* = \frac{dU}{dA} = \frac{1}{B}\frac{dU/dN}{da/dN} \tag{2}$$

where $dA$ is the incremental increase in area of the fracture surface, which equals to $Bda$. $U$ is the amount of energy dissipated in the crack propagation, that can be defined as:

$$U = \frac{1}{2}P_{max,N}\delta_{max,N} \tag{3}$$

where $P_{max,N}$ and $\delta_{max,N}$ are the maximum load and displacement at cycle number $N$, respectively. $G^*$ can be physically interpreted as fatigue resistance energy of the DCB specimens.

The fracture surface and side-view of the DCB specimens were analysed using a laser microscope (VK-X1000 from KEYENCE Corporation) to investigate the crack propagation path. The fracture surfaces were also imaged using a scanning electron microscope (SEM, JOEL JSM-7500F) to study the toughening mechanisms of the veils.

## 3. Results and discussion

### 3.1. FDG of the UD laminates

Fig. 1 presents Paris relations between $da/dN$ and $G_{Imax}$ for the interleaved UD laminates. In Fig. 1 and the rest of this paper, the interleaved laminates are referred to as the type of the laminate system followed by the type of the interlayer material, e.g. UD/PPS10 represents the UD laminate interleaved with 10 g/m$^2$ PPS veils and UD/PPS10(UV) means the corresponding PPS veils were UV-treated. From Fig. 1 (a), it was observed that the resistance curves shifted to the right due to interlaying thermoplastic veils in all cases, indicating improved FDG resistance of the laminates. The areal density of the PA veils had negligible effects on the fatigue resistance of the UD laminates. However, the fatigue resistance improved as the areal density of the PPS veils increased from 5 g/m$^2$ to 15 g/m$^2$. The gradients of the Paris relation curves, which reflect the sensitivity of the crack growth rate to the change of cyclic load [30], became smaller upon interlaying thermoplastic veils, especially for the PPS veils. This means that the interleaved UD laminates were less sensitive to fatigue crack growth, and hence possessed a longer fatigue life than the reference laminate. The curves in Fig. 1 (b) showed that an improved PPS veil/epoxy adhesion upon the UV treatment failed to further improve the fatigue delamination resistance of the UD laminates. It even caused noticeably negative effects to the fatigue life of the UD/PPS5 laminate.

To quantify the effectiveness of interlay toughening, the fatigue resistance energy ($G^*$) of the UD laminates are summarised in Fig. 2. A value of 133 J/m$^2$ was measured for $G^*$ of the reference UD laminate. Interlaying PA10 and PA15 veils significantly increased $G^*$ to 277 J/m$^2$

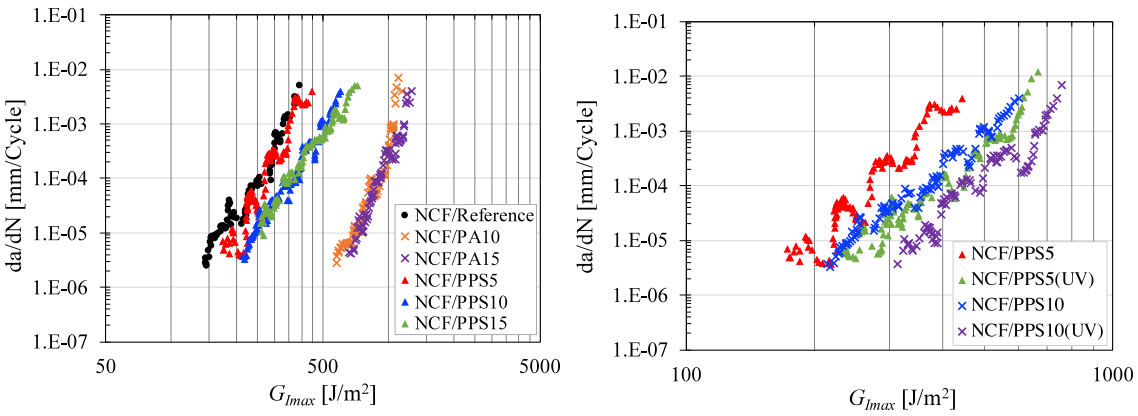


(a) Original veils (b) Effects of UV treatment

**Fig. 4.** The Paris representation of FDG of the interleaved NCF laminates.

and 292 J/m$^2$, respectively. This corresponded to an increase of 109% and 120%, respectively. $G^*$ gradually increased as the areal density of the PPS veils increased to 15 g/m$^2$, and a maximum value of 322 J/m$^2$ was obtained for the UD/PPS15 laminate, corresponding to an increase of 143%. The application of UV treatment to the PPS veils reduced $G^*$ by 15.7% for the UD/PPS5 laminate and had negligible effects on $G^*$ of the UD/PPS10 laminate.

Fig. 3 shows representative images of the fatigue fracture surface and side-view of the DCB specimens for the UD laminates. The red dashed boxes in Fig. 3 (b) indicate the interlayers after fatigue failure. Fig. 3 (a) shows that both sides of the fracture surfaces of the interleaved UD laminates were covered with a mixture of thermoplastic fibres and epoxy matrix in all cases. This corresponded to the observation in Fig. 3 (b) that the crack-path was located essentially at the middle of the interlayers. Hence, the FDG took place cohesively inside the thermoplastic interlayers for all the interleaved UD laminates.

### 3.2. FDG of the NCF laminates

The Paris relations between $da/dN$ and $G_{Imax}$ for the interleaved NCF laminates are shown in Fig. 4. It was observed that the resistance curves significantly shifted to the right upon interlaying PA veils, indicating very good toughening performance. Additionally, the areal density of the PA veils had negligible effects on the resistance to the FDG. Interleaving 5 g/m$^2$ PPS veils to the NCF laminate shifted the Paris relation curve slightly to the right, and further right-shift of the curves took place by increasing the areal density of PPS veils to 10 and 15 g/m$^2$. In contrast to the UD laminates, the enhancement of the PPS veils/epoxy adhesion upon UV-treatment obviously improved the fatigue resistance of the NCF laminates, as shown in Fig. 4 (b).

Fig. 5 presents the fatigue resistance energy of the NCF laminates. Interlaying PA veils significantly increased $G^*$ from 352 J/m$^2$ of the NCF reference laminate to around 1020 J/m$^2$ (by 190%) of both the NCF/PA10 and NCF/PA15 laminates. The improvements in $G^*$ due to interlaying PPS veils were less prominent than the PA veils. The addition of PPS veils increased $G^*$ to 393 J/m$^2$ (by 12%) of the NCF/PPS5 laminate, 515 J/m$^2$ (by 46%) of the NCF/PPS10 laminate, and further to 590 J/m$^2$ (by 67%) of the NCF/PPS15 laminate. $G^*$ of the NCF/PPS5(UV) and NCF/PPS10(UV) laminates were more or less the same, i.e. around 570 J/m$^2$, which were higher than their counterparts that were interleaved with non-treated PPS veils.

Typical photographs of the fatigue fracture surface and side-view of the DCB specimens for the NCF laminates are shown in Fig. 6. The red dashed boxes in Fig. 6 (b) indicate the interlayers after fatigue failure. It was observed that the fracture surfaces of the NCF/PA10 laminate possessed many delaminated carbon fibre bundles, which covered the white colour stitching yarn of the carbon fibre fabric, see Fig. 6 (a). The delamination of carbon fibre bundles corresponded to the observation in Fig. 6 (b) that the fracture path of the NCF/PA10 laminate was located outside of the interlayers. Hence, the FDG of the NCF/PA laminates was a mixture of carbon fibre delamination and cohesive failure inside the interlayers. Fig. 6 (b) shows that the crack path was located within the interlayers for the NCF/PPS10 and NCF/PPS10(UV) laminates, resulting in the presence of numerous PPS fibres on both sides of the corresponding fracture surfaces in Fig. 6 (a).

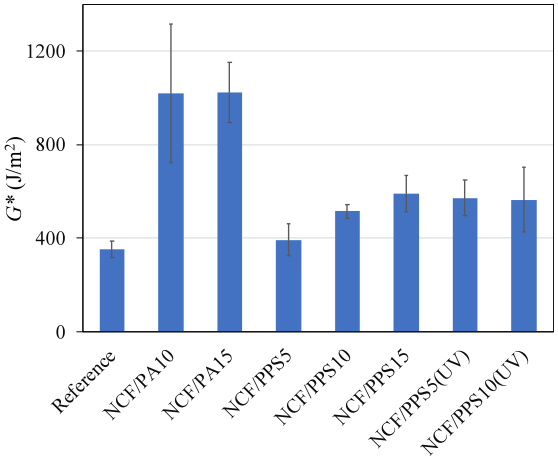


**Fig. 5.** Fatigue resistance energy ($G^*$) of the interleaved NCF laminates.

### 3.3. Toughening mechanisms and discussion

To investigate the toughening mechanisms of the thermoplastic veils, SEM analysis was carried out on the fracture surfaces of the DCB specimens, as shown in Fig. 7. The yellow arrows in Figs. 7 (a) and (c) indicate broken carbon fibres and fractured PA fibres, respectively. Fig. 7 (a) shows that all the carbon fibres on the fracture surface of the UD reference laminate were covered with epoxy resin, with a number of them having fractured. This indicates good carbon fibre/epoxy interface adhesion within the UD/Reference laminate. Hence, the main damage mechanisms of the UD reference laminate were epoxy cracking and carbon fibre breakage. Many long pulled-out and broken carbon fibres were observed on the fracture surfaces of the NCF reference laminate, see Fig. 7 (b). This was caused by significant carbon fibre debonding, bridging and breakage during the fatigue delamination process. These mechanisms and epoxy cracking were the main fracture

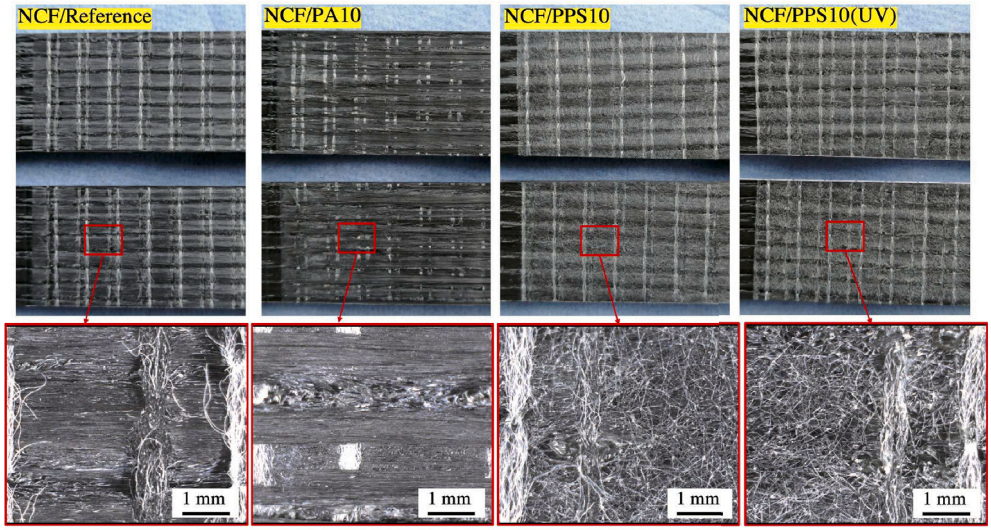


(a) Photos of the fracture surface

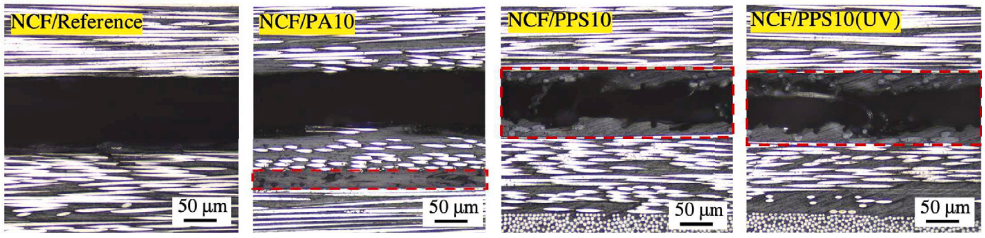


(b) Side view of the crack path

**Fig. 6.** Typical photographs of the fatigue fracture surface and side-view of the crack path of the NCF laminates. The red dashed boxes in (b) indicate the interlayers.

mechanisms of the NCF reference laminate. While different fracture mechanisms were observed for the UD and NCF reference laminates, the corresponding toughening mechanisms of the thermoplastic veils were also different.

Representative SEM images of the interleaved UD laminates are shown in Figs. 7 (c), (d) and (e). From Figs. 7 (c), it was observed that the PA resin remained in a linear shape (instead of fully mixing with the surrounding epoxy matrix) even though they melted during the laminate curing process. The high toughness of the PA resin embedded in the epoxy caused crack deflection during the FDG, that subsequently resulted in the bumps of fractured epoxy matrix and PA resin on the fracture surfaces, as shown in Fig. 7 (c). These observations indicate that the main toughening mechanisms of the PA veils were plastic deformation and fracture of the PA resin and associated crack deflection. Fig. 7 (d) shows that the failure surfaces of the UD/PPS10 laminate were covered with a large number of long PPS fibres that debonded from the epoxy matrix. Moreover, no obvious damage, such as breakage or split, to the PPS fibres was observed, indicating relatively low PPS fibre/epoxy adhesion. Accordingly, the main toughening mechanism of the PPS fibres was fibre bridging, that contributed to the right-shifts and the reduced gradients of the Paris relation curves in Fig. 1 (a) due to interleaving PPS veils. A large number of PPS fibres were also observed on the fracture surfaces of the UD/PPS10(UV) laminate, as shown in Fig. 7 (e). However, all the PPS fibres were well-embedded in the epoxy matrix, clearly indicating an improved PPS/epoxy adhesion upon the UV-treatment. Although this increased the resistance of the PPS fibres from peeling-off, it also inhibited a PPS fibre bridging mechanism. This explains why improved PPS/epoxy adhesion by UV-treatment failed to further improve the fatigue resistance of the interleaved UD laminates in Fig. 1 (b).

Figs. 7 (f), (g) and (h) present representative SEM images of the interleaved NCF laminates. Unlike the UD/PA10 laminates, the PA veils in the NCF/PA10 laminate melted and fully mixed with the epoxy matrix during the laminate curing process, see Fig. 7 (f). Accordingly, obvious plastic deformation of the mixture of the epoxy matrix and the PA resin took place during the FDG, that increased the energy dissipation of the matrix cracking mechanism. Moreover, the toughness improvement of the matrix subsequently resulted in additional carbon fibre debonding, bridging and breakage, evidenced by the presence of a larger number of pulled-out and broken carbon fibres in Fig. 7 (f) than in Fig. 7 (b). These phenomena together contributed to the significantly improved fatigue resistance upon adding PA veils, that was observed in Fig. 4 (a). The fracture surface of the NCF/PPS10 laminate in Fig. 7 (g) appeared similar to that of the UD/PPS10 laminates, i.e. featured many long pulled-out PPS fibres that were not damaged. Hence, PPS fibre debonding and bridging mechanisms also occurred during the FDG of the NCF/PPS10 laminate, that improved the fatigue delamination resistance. However, a comparison between Figs. 7 (b) and (g) showed that the addition of PPS veils to the NCF laminates fully prohibited the debonding, bridging and breakage of carbon fibres. This caused detrimental effects to the fatigue delamination resistance of the laminate, and negatively affected the overall toughening performance of the PPS veils. The application of UV treatment to the PPS veils increased the PPS/matrix interface adhesion, resulting in an obvious split and breakage of the PPS fibres on the fracture surfaces of the NCF/PPS10(UV) laminate, see Fig. 7 (h). This further enhanced the fatigue delamination resistance of the PPS veil interleaved laminate, as shown in Fig. 4 (b).

Based on the observations in this study, it is obvious that the toughening mechanisms of thermoplastic veils for the fatigue delamination resistance of the laminates were affected by the form of the

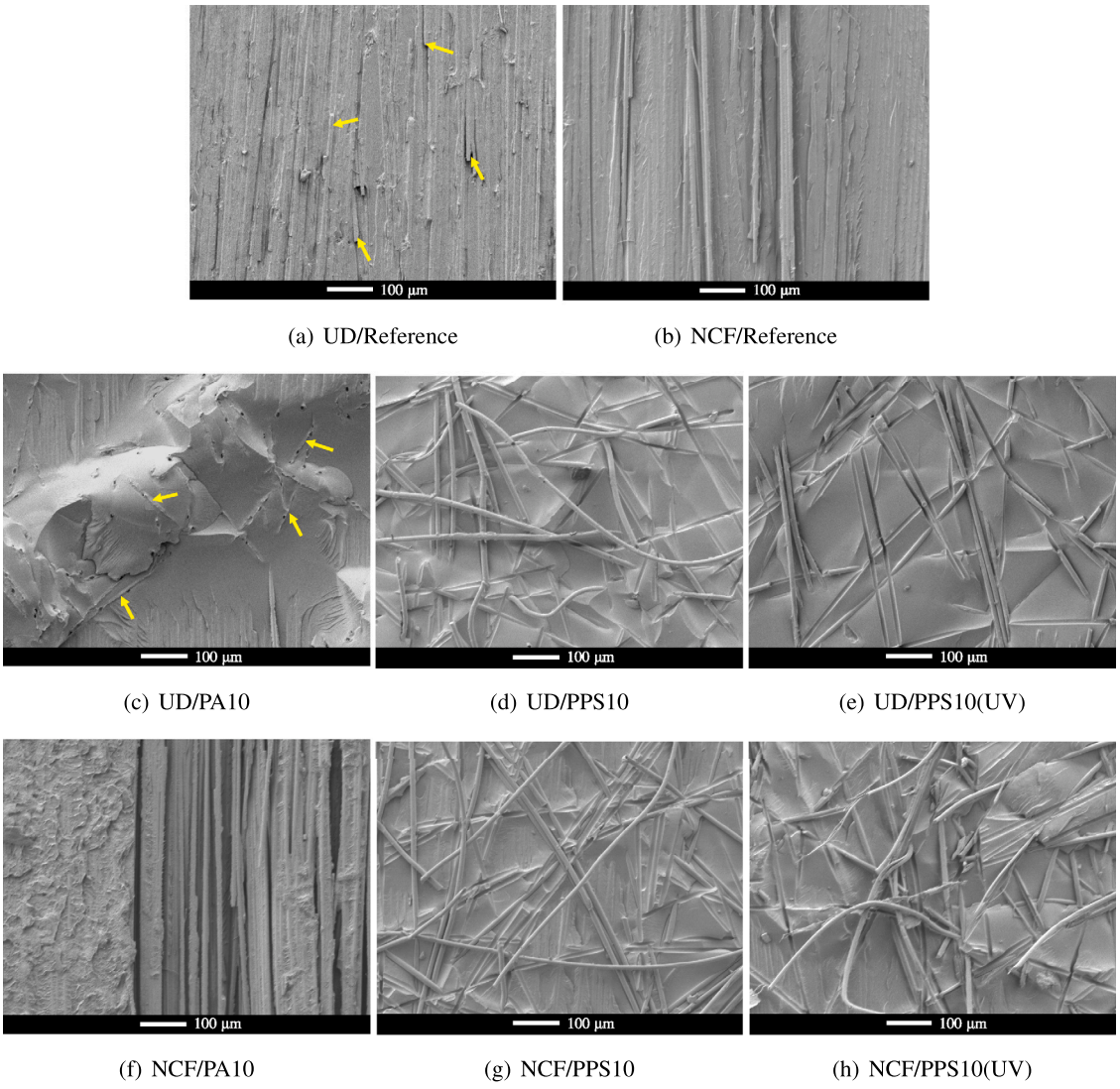


**Fig. 7.** Representative SEM images of fatigue fracture surface of the DCB specimens. The yellow arrows in (a) and (c) indicate a number of fractured carbon fibres and PA fibres, respectively.

thermoplastic veils in the laminates (melted PA fibres and non-meltable PPS fibres), the fracture mechanisms of the reference laminates and the adhesion/miscibility between the thermoplastic veils and the epoxy. It should be pointed out that the adhesion/miscibility between the thermoplastic veils and the epoxy also proved to be an important factor in the fracture behaviour of the interleaved laminates under static loading conditions in our previous work [27]. It depends on the surface activity of the thermoplastic veils and the laminate processing methods, i.e. prepreg for the UD laminates, and RTM for the NCF laminates in this study. Since the same veils were used for the UD and NCF laminates, the different laminate processing methods between the UD and NCF laminates was the main factor that could cause different veil/epoxy miscibility. This was because the partially cured (B-stage) epoxy matrix in the UD prepreg is expected to have poorer miscibility with the veils than the epoxy monomer used for the RTM process of the NCF laminates. This explained why the PA fibres melted and remained linear in shape in the UD/PA10 laminate (see Figs. 7 (c)), but fully mixed with the epoxy matrix within the NCF/PA10 laminate (see Figs. 7 (f)). However, to fully understand this issue, further study using the same epoxy matrix but at different curing stages before veil insertion and final laminate curing is still needed.

## 4. Conclusions

This work studied the effects of interleaving thermoplastic veils into carbon fibre/epoxy composites on the Mode-I fatigue delamination behaviour of the laminates using DCB specimens. Two types of laminates, i.e. unidirectional (UD) and non-crimp fabric (NCF) laminates manufactured by a prepreg and resin transfer moulding process, respectively, were interleaved by meltable PA veils and non-meltable PPS veils. The experimental results showed that adding thermoplastic veils into the laminates obviously improved the fatigue life, and also significantly increased the fatigue resistance energy ($G^*$) of the DCB specimens in all cases. For instance, $G^*$ was maximumly increased by 143% and 190% for the UD and NCF laminates, respectively. In general, the areal density of the PA veils, which melted during the laminate curing process had negligible effects on the fatigue resistance of the laminates, and the toughening performance of the non-meltable PPS veils improved with increasing areal density. The toughening mechanisms of the thermoplastic veils on the laminates have also been investigated. It was revealed that the toughening mechanisms of the thermoplastic veils were affected by the form of the thermoplastic veils in the laminates (melted PA fibres and non-meltable PPS fibres), the fracture mechanisms of the reference laminates and the adhesion/miscibility between the thermoplastic veils and the epoxy.

## Declaration of competing interest

The authors declare that they have no known competing financial interests or personal relationships that could have appeared to influence the work reported in this paper.

## Data availability

The raw/processed data required to reproduce these findings cannot be shared at this time due to legal or ethical reasons.

## Acknowledgements

Dong Quan received funding from the European Union's Horizon 2020 research and innovation programme under the Marie Skłodowska-Curie grant agreement No. 842467. The financial support from the Irish Composites Centre is also acknowledged. We would like to thank Bombardier Aerospace (UK) and Technical Fibre Products (UK) for supplying the carbon fibre fabrics and thermoplastic veils.

## References

[1] Zhou H, Du X, Liu H-Y, Zhou H, Zhang Y, Mai Y-W. Delamination toughening of carbon fiber/epoxy laminates by hierarchical carbon nanotube-short carbon fiber interleaves. Compos Sci Technol 2017;140:46–53. http://dx.doi.org/10.1016/j.compscitech.2016.12.018.

[2] Ou Y, González C, Vilatela JJ. Understanding interlaminar toughening of unidirectional CFRP laminates with carbon nanotube veils. Composites B 2020;201:108372. http://dx.doi.org/10.1016/j.compositesb.2020.108372.

[3] Quan D, Flynn S, Artuso M, Murphy N, Rouge C, Ivankovic A. Interlaminar fracture toughness of CFRPs interleaved with stainless steel fibres. Compos Struct 2019;210:49–56. http://dx.doi.org/10.1016/j.compstruct.2018.11.016.

[4] Cheng C, Zhang C, Zhou J, Jiang M, Sun Z, Zhou S, et al. Improving the interlaminar toughness of the carbon fiber/epoxy composites via interleaved with polyethersulfone porous films. Compos Sci Technol 2019;183:107827. http://dx.doi.org/10.1016/j.compscitech.2019.107827.

[5] Quan D, Alderliesten R, Dransfeld C, Murphy N, Ivanković A, Benedictus R. Enhancing the fracture toughness of carbon fibre/epoxy composites by interleaving hybrid meltable/non-meltable thermoplastic veils. Compos Struct 2020;252:112699. http://dx.doi.org/10.1016/j.compstruct.2020.112699.

[6] Beylergil B, Tanoğlu M, Aktaş E. Enhancement of interlaminar fracture toughness of carbon fiber/epoxy composites using polyamide-6,6 electrospun nanofibers. J Appl Polym Sci 2017;134(35):45244. http://dx.doi.org/10.1002/app.45244.

[7] Beylergil B, Tanoğlu M, Aktaş E. Effect of polyamide-6,6 (PA 66) nonwoven veils on the mechanical performance of carbon fiber/epoxy composites. Compos Struct 2018;194:21–35. http://dx.doi.org/10.1016/j.compstruct.2018.03.097.

[8] Beylergil B, Tanoglu M, Aktas E. Mode-I fracture toughness of carbon fiber/epoxy composites interleaved by aramid nonwoven veils. Steel Compos Struct 2019;31(2):113–23. http://dx.doi.org/10.12989/scs.2019.31.2.113.

[9] Palazzetti R, Zucchelli A, Gualandi C, Focarete M, Donati L, Minak G, et al. Influence of electrospun Nylon 6,6 nanofibrous mats on the interlaminar properties of Gr-epoxy composite laminates. Compos Struct 2012;94(2):571–9. http://dx.doi.org/10.1016/j.compstruct.2011.08.019.

[10] Palazzetti R, Zucchelli A, Trendafilova I. The self-reinforcing effect of Nylon 6,6 nano-fibres on CFRP laminates subjected to low velocity impact. Compos Struct 2013;106:661–71. http://dx.doi.org/10.1016/j.compstruct.2013.07.021.

[11] Saghafi H, Zucchelli A, Palazzetti R, Minak G. The effect of interleaved composite nanofibrous mats on delamination behavior of polymeric composite materials. Compos Struct 2014;109:41–7. http://dx.doi.org/10.1016/j.compstruct.2013.10.039.

[12] Brugo T, Palazzetti R. The effect of thickness of Nylon 6,6 nanofibrous mat on modes I–II fracture mechanics of UD and woven composite laminates. Compos Struct 2016;154:172–8. http://dx.doi.org/10.1016/j.compstruct.2016.07.034.

[13] Palazzetti R, Zucchelli A. Electrospun nanofibers as reinforcement for composite laminates materials-a review. Compos Struct 2017;182:711–27. http://dx.doi.org/10.1016/j.compstruct.2017.09.021.

[14] Wong DW, Lin L, McGrail PT, Peijs T, Hogg PJ. Improved fracture toughness of carbon fibre/epoxy composite laminates using dissolvable thermoplastic fibres. Composites A 2010;41(6):759–67. http://dx.doi.org/10.1016/j.compositesa.2010.02.008.

[15] Molnar K, Kostakova E, Meszaros L. The effect of needleless electrospun nanofibrous interleaves on mechanical properties of carbon fabrics/epoxy laminates. EXPRESS Polym Lett 2014;8(1):62–72. http://dx.doi.org/10.3144/expresspolymlett.2014.8.

[16] Beylergil B, Tanoglu M, Aktaş E. Modification of carbon fibre/epoxy composites by polyvinyl alcohol (PVA) based electrospun nanofibres. Adv Compos Lett 2016;25(3):69–76. http://dx.doi.org/10.1177/096369351602500303.

[17] Beckermann GW, Pickering KL. Mode I and mode II interlaminar fracture toughness of composite laminates interleaved with electrospun nanofibre veils. Composites A 2015;72:11–21. http://dx.doi.org/10.1016/j.compositesa.2015.01.028.

[18] Beckermann GW. Nanofiber interleaving veils for improving the performance of composite laminates. Reinf Plast 2017;61(5):289–93. http://dx.doi.org/10.1016/j.repl.2017.03.006.

[19] Daelemans L, van der Heijden S, Baere ID, Rahier H, Paepegem WV, Clerck KD. Nanofibre bridging as a toughening mechanism in carbon/epoxy composite laminates interleaved with electrospun polyamide nanofibrous veils. Compos Sci Technol 2015;117:244–56. http://dx.doi.org/10.1016/j.compscitech.2015.06.021.

[20] Kuwata M, Hogg P. Interlaminar toughness of interleaved CFRP using non-woven veils: Part 1. Mode-I testing. Composites A 2011;42(10):1551–9. http://dx.doi.org/10.1016/j.compositesa.2011.07.016.

[21] Kuwata M, Hogg P. Interlaminar toughness of interleaved CFRP using non-woven veils: Part 2. Mode-II testing. Composites A 2011;42(10):1560–70. http://dx.doi.org/10.1016/j.compositesa.2011.07.017.

[22] Daelemans L, van der Heijden S, Baere ID, Rahier H, Van Paepegem W, Clerck KD. Improved fatigue delamination behaviour of composite laminates with electrospun thermoplastic nanofibrous interleaves using the central Cut-Ply method. Composites A 2017;94:10–20. http://dx.doi.org/10.1016/j.compositesa.2016.12.004.

[23] Brugo T, Minak G, Zucchelli A, Saghafi H, Fotouhi M. An investigation on the fatigue based delamination of woven carbon-epoxy composite laminates reinforced with polyamide nanofibers. Procedia Eng 2015;109:65–72. http://dx.doi.org/10.1016/j.proeng.2015.06.208.

[24] Brugo T, Minak G, Zucchelli A, Yan X, Belcari J, Saghafi H, et al. Study on mode I fatigue behaviour of Nylon 6,6 nanoreinforced CFRP laminates. Compos Struct 2017;164:51–7. http://dx.doi.org/10.1016/j.compstruct.2016.12.070.

[25] Quan D, Bologna F, Scarselli G, Ivankovic A, Murphy N. Interlaminar fracture toughness of aerospace-grade carbon fibre reinforced plastics interleaved with thermoplastic veils. Composites A 2020;128:105642. http://dx.doi.org/10.1016/j.compositesa.2019.105642.

[26] Quan D, Bologna F, Scarselli G, Ivanković A, Murphy N. Mode-II fracture behaviour of aerospace-grade carbon fibre/epoxy composites interleaved with thermoplastic veils. Compos Sci Technol 2020;191:108065. http://dx.doi.org/10.1016/j.compscitech.2020.108065.

[27] Quan D, Deegan B, Alderliesten R, Dransfeld C, Murphy N, Ivanković A, et al. The influence of interlayer/epoxy adhesion on the Mode-I and Mode-Ii fracture response of carbon fibre/epoxy composites interleaved with thermoplastic veils. Mater Des 2020;192:108781. http://dx.doi.org/10.1016/j.matdes.2020.108781.

[28] ASTM Standard D5528-13(2013). Standard test method for mode I interlaminar fracture toughness of unidirectional fiber-reinforced polymer matrix composites, ASTM international. ASTM; 2013.

[29] ASTM Standard E647-15(2015). Standard test method for measurement of fatigue crack growth rates, ASTM international. ASTM; 2015.

[30] Tsai S-N, Carolan D, Sprenger S, Taylor AC. Fracture and fatigue behaviour of carbon fibre composites with nanoparticle-sized fibres. Compos Struct 2019;217:143–9. http://dx.doi.org/10.1016/j.compstruct.2019.03.015.